Table 1. PrPC-interacting proteins (PrPIPs) identified by protein microarray analysis

No.	*Entrez gene ID*	*Gene symbol*	*Gene name*	*Putative molecular function*	*Block*	*Row*	*Column*	*Z-score*	*Gene expression in adult mouse brain (region with the highest expression level)*
1	54478	FAM64A	Family with sequence similarity 64, member A	A protein with the DUF1466 domain of unknown function	20	11	7, 8	21.89656	Unknown
2	3198	HOXA1	Homeobox A1	A transcription factor that regulates the placement of hindbrain segments in the proper location along the anterior–posterior axis during development	35	11	3, 4	18.36074	Yes (CB)
3	1448	CSN3	Casein kappa	A milk protein	20	9	9, 10	12.58106	Yes (OLF)
4	29994	BAZ2B	Bromodomain adjacent to zinc finger domain, 2B	A component of chromatin remodeling complexes	24	10	5, 6	7.96988	Yes (MY)
5	84310	C7orf50	Chromosome 7 open reading frame 50	A hypothetical protein of unknown function	21	11	9, 10	6.7938	Unknown
6	6835	SURF2	Surfeit 2	The housekeeping gene of unknown function	15	9	15, 16	6.31368	Yes (MY)
7	79005	SCNM1	Sodium channel modifier 1	A zinc finger protein acting as a premRNA splicing factor	18	6	3, 4	6.06453	Yes (CB and other regions)
8	494514	C18orf56	Chromosome 18 open reading frame 56	A hypothetical protein of unknown function	10	10	19, 20	6.02515	Unknown
9	1263	PLK3	Polo-like kinase 3 (Drosophila)	A serine/threonine kinase that regulates cell cycle progression	34	13	13, 14	5.94109	Yes (MY)
10	55696	RBM22	RNA binding motif protein 22	A zinc finger protein with the RNA recognition motif of unknown function	20	9	7, 8	5.67225	Yes (CB)
11	91050	DKFZp761B107	Hypothetical protein DKFZp761B107	A protein with the SMC N-terminal domain of unknown function	22	12	3, 4	5.36251	Unknown
12	4350	MPG	N-methylpurine-DNA glycosylase	A DNA glycosylase acting as a DNA repair enzyme	37	9	11, 12	5.16637	Yes (RHP)
13	7745	ZNF192	Zinc finger protein 192	A Kruppel family zinc finger transcription factor	21	11	13, 14	5.12927	Unknown
14	85480	TSLP	Thymic stromal lymphopoietin	A haemopoietic cytokine that enhances the maturation of dendritic cells	21	10	19, 20	4.92555	Yes (RHP)
15	51202	DDX47	DEAD (Asp-Glu-Ala-Asp) box polypeptide 47	A member of the DEAD box protein family RNA helicases	2	11	11, 12	4.90132	Yes (MY)
16	57787	MARK4	MAP/microtubule affinity-regulating kinase 4	A serine/threonine kinase that regulates microtubule organization in neuronal cells	12	13	5, 6	4.38333	Yes (TH)
17	79797	ZNF408	Zinc finger protein 408	A zinc finger protein with the SFP1 domain acting as a transcriptional repressor that regulates cell cycle	21	11	19, 20	4.27504	Unknown

18	9519	TBPL1	TBP-like 1	A general transcription factor that regulates spermatogenesis	3	12	1, 2	4.16447	Yes (OLF)
19	29777	ABT1	Activator of basal transcription 1	A basal transcriptional activator	36	9	15, 16	3.97136	Yes (OLF)
20	6171	RPL41	Ribosomal protein L41	A componet of the 60S ribosome subunit	14	10	7, 8	3.9388	Unknown
21	283337	ZNF740	Zinc finger protein 740	A zinc finger protein of unknown function	20	9	15, 16	3.88503	Unknown
22	51503	CWC15	CWC15 homolog (S. cerevisiae)	A cell cycle control protein involved in mRNA splicing	19	7	13, 14	3.78582	Unknown
23	2273	FHL1	Four and a half LIM domain 1	A protein with the LIM domain that regulates skeletal muscle differentiation	26	3	11, 12	3.75175	Yes (sAMY)
24	65062	ALS2CR4	Amyotrophic lateral sclerosis 2 (juvenile) chromosome region, candidate 4	A membrane protein of unknown function	34	7	7, 8	3.69722	Yes (RHP)
25	8870	IER3	Immediate early response 3	The immediate early gene acting as an antiapoptosis regulator	26	10	13, 14	3.6018	Yes (CB)
26	57179	KIAA1191	KIAA1191	A cytoplasmic protein of unknown function	10	10	13, 14	3.56924	Unknown
27	138428	PTRH1	Peptidyl-tRNA hydrolase 1 homolog (S. cerevisiae)	A peptidyl-tRNA hydrolase	47	10	19, 20	3.55258	Yes (CTX)
28	9659	PDE4DIP	Phosphodiesterase 4D interacting protein (myomegalin)	A protein of the golgi/centrosome that interacts with a cyclic nucleotide phosphodiesterase	25	11	1, 2	3.54046	Yes (HIP)
29	55843	ARHGAP15	Rho GTPase activating protein 15	A Rho GTPase-activating protein acting as a regulator of RAC1	9	6	13, 14	3.50411	Yes (CTX)
30	92170	MTG1	Mitochondrial GTPase 1 homolog (S. cerevisiae)	A mitochondrial GTPase	48	14	7, 8	3.49729	Yes (HIP)
31	84916	CIRH1A	Cirrhosis, autosomal recessive 1 A (cirhin)	A mitochondrial protein with WD40 repeats of unknown function	14	10	19, 20	3.4511	Yes (HIP)
32	26523	EIF2C1	Eukaryotic translation initiation factor 2C, 1	A member of the Argonaute family (AGO1) that plays a role in siRNA-mediated gene silencing	18	11	11, 12	3.43671	Yes (HIP)
33	11091	WDR5	WD repeat domain 5	A protein with WD40 repeats that constitutes a component of histone methyltransferase complexes	20	7	9, 10	3.37083	Yes (HIP)
34	55803	CENTA2	Centaurin, alpha 2	A plasma membrane GTPase activating protein with PH domains	47	12	5, 6	3.25269	Yes (MY)
35	94274	PPP1R14 A	Protein phosphatase 1, regulatory (inhibitor) subunit 14 A	A phosphorylation-dependent inhibitor of smooth muscle myosin phosphatase	9	5	3, 4	3.25117	Yes (MY)
36	1153	CIRBP	Cold-inducible RNA binding protein	A cold stress-inducible protein wuth the RNA recognition motif that plays a role in cold-induced suppression of cell proliferation	16	10	3, 4	3.22391	Yes (CTX)

Table 1. (*Continued*)

No.	Entrez gene ID	Gene symbol	Gene name	Putative molecular function	Block	Row	Column	Z-score	Gene expression in adult mouse brain (region with the highest expression level)
37	57732	ZFYVE28	Zinc finger, FYVE domain containing 28	An endosomal protein with the FYVE domain that targets proteins to membrane lipids via interaction with PI3P	12	10	11,12	3.20574	Yes (CB and other regions)
38	84305	WIBG	Within bgcn homolog (Drosophila)	A protein with the Mogo-bind domain of unknown function	43	9	15,16	3.19741	Yes (OLF)
39	55651	NOLA2	Nucleolar protein family A, member 2 (H/ACA small nucleolar RNPs)	A member of the H/ACA snoRNPs gene family that regulates rRNA processing and modification	15	6	15,16	3.155	Yes (OLF)
40	8495	PPFIBP2	PTPRF interacting protein, binding protein 2 (liprin beta 2)	A protein with SAM domains acting as a scaffold for recruitment and anchoring of LAR family PTPases	47	12	11,12	3.13682	Yes (MY)
41	286301	FAM27E3	Family with sequence similarity 27, member E3	A protein of unknown function	14	11	9,10	3.11032	Unknown
42	2258	FGF13	Fibroblast growth factor 13	A member of the FGF family that plays a role in neuronal development	35	11	17,18	3.1035	Yes (HIP)
43	150209	AIFM3	Apoptosis-inducing factor, mitochondrion-associated, 3	A mitochondrial protein with the Rieske domain and the pyridine nucleotide-disulphide oxidoreductase domain acting as an apoptosis inducer	42	10	15,16	3.09063	Unkown
44	1267	CNP	2′,3′-cyclic nucleotide 3′ phosphodiesterase	A cyclic nucleotide phosphodiesterase serving as a marker of myelin	20	10	19,20	3.07624	Yes (CB and other regions)
45	28987	NOB1	NIN1/RPN12 binding protein 1 homolog (S. cerevisiae)	A protein with the PUN domain and the zinc ribbon domain acting as a ribonuclease	14	11	17,18	3.06336	Yes (CB and other regions)
46	55599	RNPC3	RNA-binding region (RNP1, RRM) containing 3	A nuclear protein with RNA recognition motifs that constitutes a component of the U12-type spliceosome	9	8	19,20	3.01035	Yes (OLF)
47	8444	DYRK3	Dual-specificity tyrosine-(Y)-phosphorylation regulated kinase 3	A DYRK family dual-specificity protein kinase that regulates caveolae trafficking	20	13	9,10	3.00278	Yes (HIP)

Among 5000 proteins on the microarray, 47 were identified as the proteins showing a significant interaction. They are listed with Entrez Gene ID, gene symbol, gene name, molecular function, the position on the array, the Z-score and the information on gene expression in the adult mouse brain, including the region with the highest expression level on the sagittal plane of the Allen Brain Atlas.

CB, cerebellum; CTX, cerebral cortex; HIP, hippocampal region; MY, medulla oblongata; OLF, olfactory bulb; sAMY, striatum-like amygdalar nuclei; TH, thalamus; RHP, retrohippocampal region.

12 genes in the adult mouse brain is currently unknown. Thus, the expression of PrPIPs is enriched in the adult mouse brain, suggesting the possible interaction of these with PrPC that is expressed broadly at high levels in neurones of the adult rodent CNS [3]. The BIND database search indicated that none of 47 PrPIPs were classified into previously reported PrPC-interacting partners.

We did not detect any negative control spots as positive, including those of BSA, calmodulin, GST, a rabbit anti-GST antibody, human IgG subclasses, an antibiotin antibody and buffer-only control, whereas we identified a battery of positive control spots as positive, such as those of an Alexa Fluor 647-labelled antibody, a biotinylated anti-mouse antibody binding to Alexa Fluor 647-conjugated anti-V5 antibody and V5 protein (Figure 1, panels b–f). The protein microarray we utilized includes only three previously reported PrPC-binding partners, such as glial fibrillary acidic protein [15], tubulin [25] and casein kinase 2 [27] (see Table S2). However, we could not identify them as a significant PrPC interactor in the present study.

Human neurones in culture expressed mRNA of PrPC interactors

Because PrPC *in vivo* is expressed at the highest level in neurones in the CNS, it is important to identify the cell types expressing PrPIPs. By reverse transcription (RT)-PCR analysis, the transcripts coding for PRNP and PR209-interacting proteins, such as FAM64A, PLK3 and MPG, were expressed widely in various human neural and non-neural cell lines (Figure 2, panels a, c, d, e, lanes 3–12). They include cultured human AS, NP cells, NTera2 teratocarcinoma-derived differentiated neurones (NTera2N), Y79 retinoblastoma, SK-N-SH neuroblastoma, IMR-32 neuroblastoma, U-373MG astrocytoma, HMO6 microglia, HeLa cervical carcinoma and HepG2 hepatocellular carcinoma cells. In contrast, high levels of HOXA1 mRNA were expressed in limited cell types, such as NTera2N, U-373MG, HeLa and HepG2 (Figure 2, panel b, lanes 3–12). High levels of PLK3, MPG and PRNP mRNAs were also identified in the human cerebral cortex (CBR) (Figure 2, panels c, d, e, lane 1). The levels of G3PDH mRNA were constant among the cells and tissues examined (Figure 2, panel f, lanes 1, 3–12). By contrast, no products were amplified, when total RNA was processed for PCR without inclusion of the RT step, excluding a contamination of genomic DNA (Figure 2, panels a–f, lane 2). Because NTera2N cells serve as a model of differentiated human neurones in culture [45], these observations suggest that FAM64A, HOXA1, PLK3 and MPG are neuronal proteins coexpressed with PrPC.

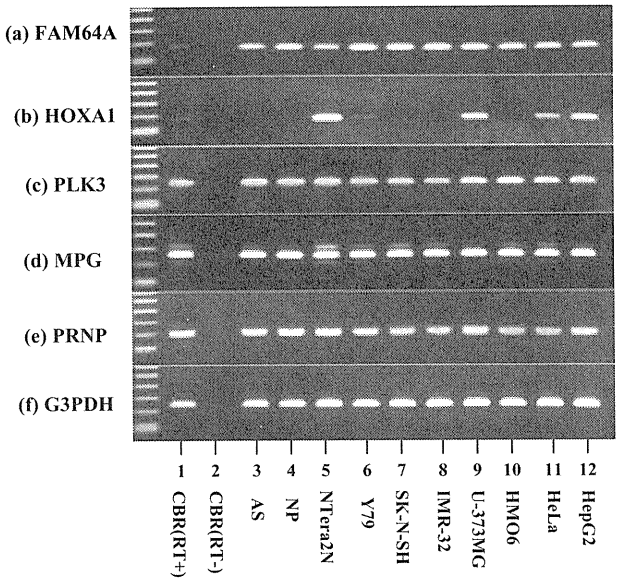

Figure 2. Expression of mRNAs of PrPC interactors in human neural cells. The expression of (a) FAM64A, (b) HOXA1, (c) PLK3, (d) MPG, (e) PRNP and (f) G3PDH mRNAs was studied in human neural and non-neural cells by RT-PCR. The lanes (1–12) represent: (1) the frontal cerebral cortex (CBR) with inclusion of the reverse transcription step (RT+), (2) CBR without inclusion of the reverse transcription step (RT–), (3) cultured astrocytes (AS), (4) cultured neuronal progenitor (NP) cells, (5) NTera2 teratocarcinoma-derived differentiated neurones (NTera2N), (6) Y79 retinoblastoma, (7) SK-N-SH neuroblastoma, (8) IMR-32 neuroblastoma, (9) U-373MG astrocytoma, (10) HMO6 microglia cell line, (11) HeLa cervical carcinoma and (12) HepG2 hepatocellular carcinoma. The DNA size marker (100-bp ladder) is shown on the left.

Validation of protein microarray data

To verify the results of protein microarray analysis, PR209 and interactors were cloned individually into distinct expression vectors, and were coexpressed transiently in HEK293 cells. FAM64A, HOXA1, PLK3 and MPG were selected for the interactors examined, because of their possible involvement in neural function (see *Discussion*). Because the antibodies suitable for immunoprecipitation with FAM64A, PLK3 and MPG are currently unavailable, we performed immunoprecipitation analysis by using the tag-specific antibodies. First, PR209 was expressed as a Flag-tagged fusion protein, whereas the interactors were

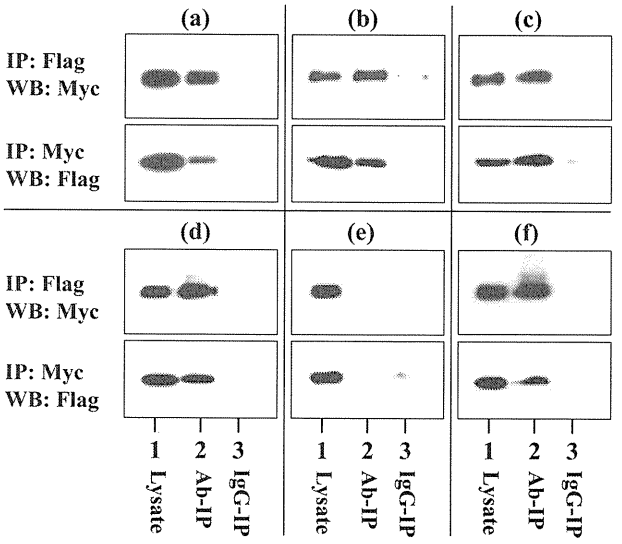

Figure 3. Coimmunoprecipitation analysis. PR209, the N-terminal (NT) half, and the C-terminal (CT) half were expressed as a Flag-tagged fusion protein, while FAM64A, HOXA1, PLK3 and MPG were expressed as a Myc-tagged fusion protein in HEK293 cells. Immunoprecipitation (IP) followed by Western blotting (WB) was performed by using the antibodies against Flag and Myc. The interaction indicates (a) PR209-FAM64A, (b) PR209-PLK3, (c) PR209-MPG, (d) PR209-HOXA1, (e) NT-HOXA1 and (f) CT-HOXA1. The lanes (1–3) represent: (1) input control of cell lysate, (2) IP with anti-Flag or anti-Myc antibody and (3) IP with normal mouse or rabbit IgG.

expressed as a Myc-tagged fusion protein. Coimmunoprecipitation and Western blot validated the interaction of PR209 with FAM64A (Figure 3a), PLK3 (Figure 3b), MPG (Figure 3c) and HOXA1 (Figure 3d). Furthermore, we found that not the N-terminal half but the C-terminal half of PR209 is bound to HOXA1 (Figure 3e,f), excluding non-specific coimmunoprecipitation of PR209 and the interactors in the transient expression system using HEK293 cells.

Next, PR209 was expressed as a DsRed-tagged fusion protein in HEK293 cells. It was located predominantly in the nucleus and the cytoplasm, and less abundantly on the plasma membrane (Figure 4, panels a, d, g, j, m). The EYFP-tagged fusion protein of FAM64A or HOXA1 was located predominantly in the nucleus, where it was colocalized with PR209 (Figure 4, panels b, c, h, i). The EYFP-tagged FAM64A protein was also located chiefly in the nucleus colocalized with DsRed-tagged PR209 in SK-N-SH cells similarly in HEK293, suggesting that the unique subcellular location of FAM64A and PR209 is not attributable to HEK293 cell-specific intracellular trafficking of the recombinant proteins (Figure 4, panels d–f). The GFP-tagged PLK3 fusion protein, expressed on the plasma membrane and in the cytoplasm, showed discernible colocalization with PR209 (Figure 4, panels k, l). The GFP-tagged MPG fusion protein was located chiefly in the nucleus, coexisting with PR209 (Figure 4, panels n, o). Thus, a substantial part of PRP209 and interactors are colocalized in specific subcellular compartments in HEK293 and SK-N-SH cells following transient expression.

Proteinase K sensitivity and detergent insolubility of PR209

To study the proteinase K-resistant property of PR209 coexpressed with the interactors in HEK293 cells, cellular protein extract was treated with proteinase K. In some experiments, the cells were exposed to MG-132 in the last 24 h before harvest. Coexpression of PR209 with HOXA1 or FAM64A did not generate proteinase K-resistant products regardless of treatment with MG-132 (Figure 5a, lanes 1–6; upper panel: HOXA1; lower panel: FAM64A). To determine the detergent-insoluble property of PR209, cellular protein extract was separated into 0.5% Nonidet P-40-soluble (S) and -insoluble (P) fractions. Unexpectedly, a great amount of the PR209 protein was recovered from the detergent-insoluble (P) fraction, even when PR209 alone without interactors was transiently expressed in HEK293 cells (Figure 5b, lanes 7, 8; upper panel: HOXA1; lower panel: FAM64A). The detergent-insoluble property of PR209 was not affected by coexpression of the interactors, such as HOXA1 or FAM64A, either in the presence or absence of MG-132 (Figure 5, lanes 9–12; upper panel: HOXA1; lower panel: FAM64A). Thus, coexpression of PR209 with the interactors did not produce proteinase K-resistant proteins, although PR209 showed an intrinsic detergent insolubility in HEK293 cells.

Molecular network analysis of PrPC interactors

Functional annotation based on DAVID showed that the great majority of PrPIPs identified by protein microarray analysis play a role in the recognition of nucleic acids, involved in regulation of diverse cellular function (Figure 6).

To identify the molecular network of PrPC and PrPIPs, we imported the list of Entrez gene IDs of 47 PrPIPs into KeyMolnet, the comprehensive biological information

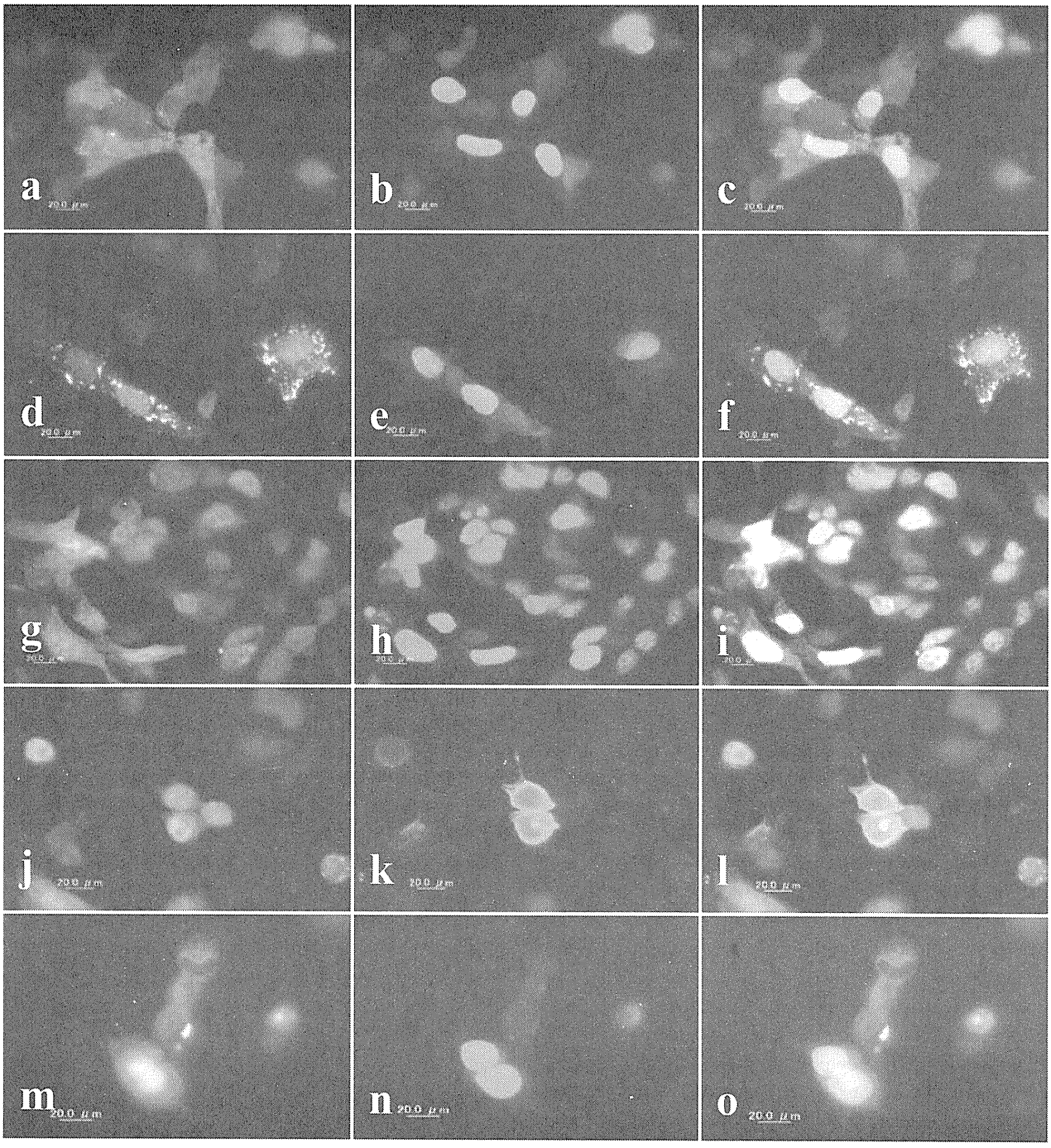

Figure 4. Cell imaging analysis. PR209 was expressed as a DsRed-tagged fusion protein, while FAM64A, HOXA1, PLK3 and MPG were expressed as an EYFP- or GFP-tagged fusion protein in HEK293 cells or in SK-N-SH cells. The panels (a–o) represent (a–c and g–o) HEK293 and (d–f) SK-N-SH of the following: (a) PR209, (b) FAM64A, (c) merge of **a** and **b**, (d) PR209, (e) FAM64A, (f) merge of **d** and **e**, (g) PR209, (h) HOXA1, (i) merge of **g** and **h**, (j) PR209, (k) PLK3, (l) merge of **j** and **k**, (m) PR209, (n) MPG and (o) merge of **m** and **n**.

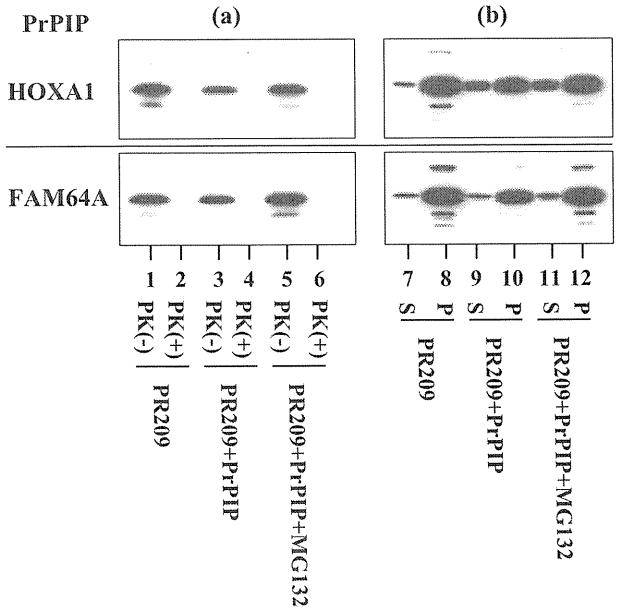

Figure 5. Biochemical property of PR209. Either Flag-tagged PR209 alone (lanes 1, 2, 7, 8) or the combination of PR209 and Myc-tagged PrPIP (lanes 3–6 and 9–12), such as HOXA1 (upper panels) or FAM64A (lower panels), were expressed in HEK293 cells. The cells were harvested at 48 h after transfection of the vectors. In some cultures, the cells were exposed to 10 μM MG-132 during the last 24 h before harvest (lanes 5, 6, 11, 12). (a) Proteinase K treatment. Total cellular protein extract was treated with (+: lanes 2, 4, 6) or without (–: lanes 1, 3, 5) 5 μg/ml proteinase K (PK) at 37°C for 30 min, and then processed for Western blot using 3F4 antibody. (b) Detergent treatment. Total cellular protein extract was separated into 0.5% Nonidet P-40-soluble (S: 50 μg of protein) and -insoluble (P: 7 μg of protein) fractions, and then processed for Western blot using 3F4 antibody.

platform of human molecules and molecular relations. It extracted 39 genes directly linked to 47 PrPIPs. Subsequently, the 'N-points to N-points' search starting from PrPC ending with 39 genes via the shortest route connecting them was performed. This generated a complex molecular network composed of 214 fundamental nodes and 579 molecular relations (Figure 7). Not surprisingly, KeyMolnet operating on the knowledgebase could not identify the direct interaction between PrPC and 47 PrPIPs, because their relationship has not been reported previously. Furthermore, KeyMolnet indicated the primary location of PrPC on the cell-surface membrane, but neither in the cytoplasm nor in the nucleus. When compared with the canonical pathways of KeyMolnet, statistical analysis indicated that the generated network has the most significant relationship with the AKT signalling pathway (the score 50.9). This was followed by the JNK signalling pathway in the second rank (the score 48.4), the MAPK signalling pathway in the third rank (the score 42.8) and the p38 signalling pathway in the fourth rank (the score 36.3). Thus, the molecular network of PrPC and interactors constitutes the key signal-transducing pathways pivotal for regulation of cell differentiation, proliferation, survival and apoptosis.

Discussion

We have performed screening of PrPIPs by using a human protein microarray containing 5000 proteins of various functional classes. By probing the array with PR209 spanning amino acid residues 23–231 of PrPC, we identified 47 novel PrPIPs. The functional annotation on the DAVID database suggested that the great majority of PrPIPs are categorized into the proteins involved in recognition of nucleic acids. The Allen Brain Atlas database search suggested that the great majority of 47 PrPIP orthologues are expressed in the adult rodent brain. Because high-throughput screening of high-density protein microarray enables us to identify a large number of putative binding partners at one time, it is often difficult to extract biological implications of their molecular relationship from such a large quantity of available data. To overcome this difficulty, we have made a breakthrough to identify the molecular network most closely associated with PrPC and the interactors by KeyMolnet, a bioinformatics tool for analysing molecular interaction on the curated knowledge database. The molecular network of PrPC and 47 PrPIPs on KeyMolnet showed an association most relevant to AKT, JNK and MAPK signalling pathways.

Advantages and limitations of protein microarray technology for identification of protein–protein interaction

Protein microarray serves as a powerful tool for the rapid and systematic identification of protein–protein and other biomolecule interactions. Protein microarray has a wide range of applications, including characterization of antibody specificity and autoantibody repertoire, and identification of novel biomarkers and molecular targets associated with disease type, stage and progression, leading to establishment of personalized medicine [47–49].

However, protein microarray technology is still under development in methodological aspects. In general,

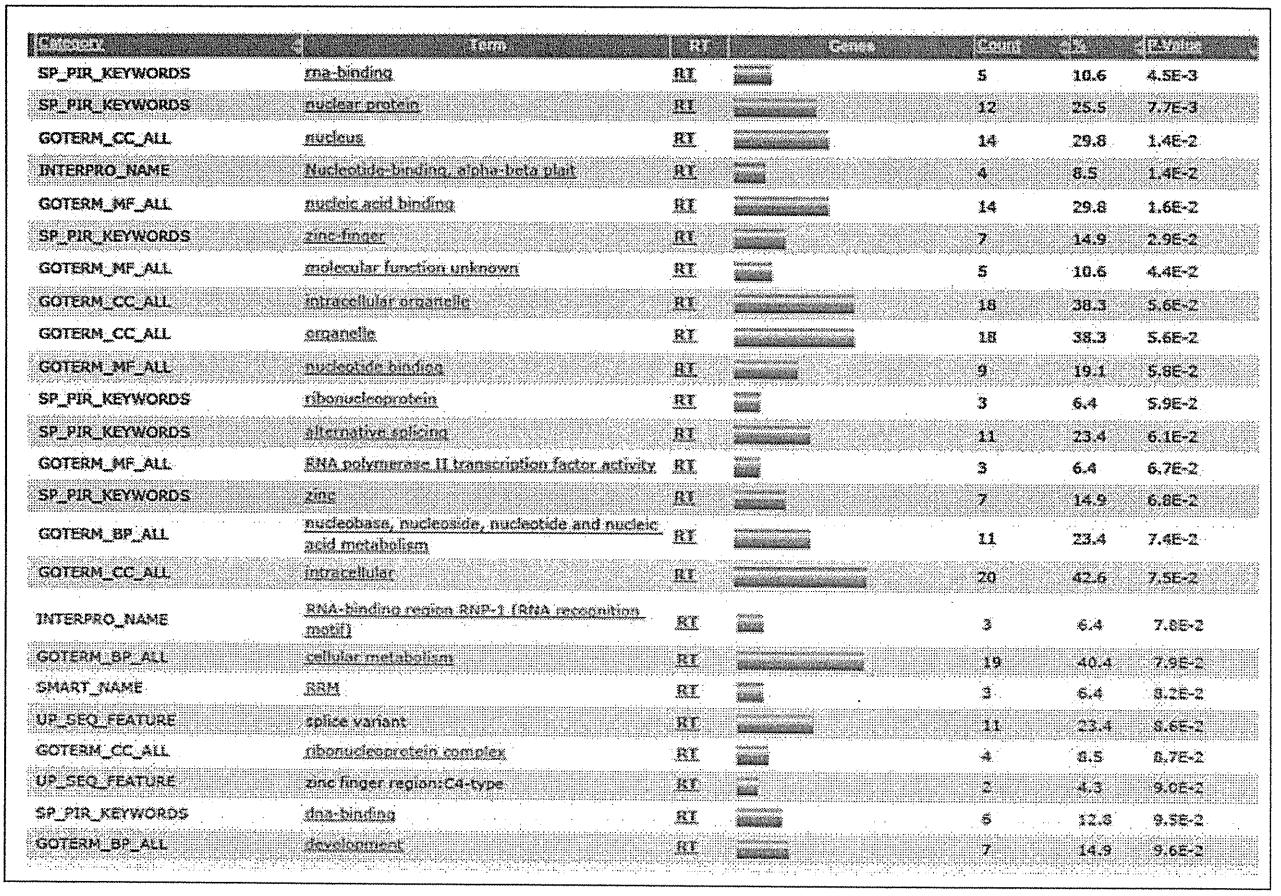

Category	Term	RT	Genes	Count	%	PValue
SP_PIR_KEYWORDS	rna-binding	RT		5	10.6	4.5E-3
SP_PIR_KEYWORDS	nuclear protein	RT		12	25.5	7.7E-3
GOTERM_CC_ALL	nucleus	RT		14	29.8	1.4E-2
INTERPRO_NAME	Nucleotide-binding, alpha-beta plait	RT		4	8.5	1.4E-2
GOTERM_MF_ALL	nucleic acid binding	RT		14	29.8	1.6E-2
SP_PIR_KEYWORDS	zinc-finger	RT		7	14.9	2.9E-2
GOTERM_MF_ALL	molecular function unknown	RT		5	10.6	4.4E-2
GOTERM_CC_ALL	intracellular organelle	RT		18	38.3	5.6E-2
GOTERM_CC_ALL	organelle	RT		18	38.3	5.6E-2
GOTERM_MF_ALL	nucleotide binding	RT		9	19.1	5.8E-2
SP_PIR_KEYWORDS	ribonucleoprotein	RT		3	6.4	5.9E-2
SP_PIR_KEYWORDS	alternative splicing	RT		11	23.4	6.1E-2
GOTERM_MF_ALL	RNA polymerase II transcription factor activity	RT		3	6.4	6.7E-2
SP_PIR_KEYWORDS	zinc	RT		7	14.9	6.8E-2
GOTERM_BP_ALL	nucleobase, nucleoside, nucleotide and nucleic acid metabolism	RT		11	23.4	7.4E-2
GOTERM_CC_ALL	intracellular	RT		20	42.6	7.5E-2
INTERPRO_NAME	RNA-binding region RNP-1 (RNA recognition motif)	RT		3	6.4	7.8E-2
GOTERM_BP_ALL	cellular metabolism	RT		19	40.4	7.9E-2
SMART_NAME	SRM	RT		3	6.4	8.2E-2
UP_SEQ_FEATURE	splice variant	RT		11	23.4	8.6E-2
GOTERM_CC_ALL	ribonucleoprotein complex	RT		4	8.5	8.7E-2
UP_SEQ_FEATURE	zinc finger region:C4-type	RT		2	4.3	9.0E-2
SP_PIR_KEYWORDS	dna-binding	RT		6	12.8	9.5E-2
GOTERM_BP_ALL	development	RT		7	14.9	9.6E-2

Figure 6. Functional annotation of PrPC interactors. Functional annotation of 47 PrPIPs identified by protein microarray analysis was performed by the program on DAVID bioinformatics database. When the list of Entrez gene IDs of 47 PrPIPs was imported, 34 genes were functionally categorized into 24 subgroups created by related databases, with enriched terms closely associated with the gene list examined. The genes excluded from the list ($n = 13$) are FAM64A, C7orf50, SCNM1, C18orf56, DKFZp761B107, TSLP, CWC15, KIAA1191, ARHGAP15, WDR5, WIBG, FAM27E3 and NOB1 (see Table 1 for the gene symbol). RT represents related term search. Genes and count indicate the genes involved in the term. The percentage is calculated from the formula following: gene involvement (%) = involved genes/total genes. *P*-value represents the *P*-value of gene enrichment analysis evaluated by the modified Fisher's exact test where it is the smaller, the genes are the more enriched in the term.

protein microarray has its own limitation associated with the expression and purification of a wide variety of target proteins. In the microarray we utilized, the target proteins were expressed in a baculovirus expression system, purified under native conditions, and spotted on to the slides to ensure the preservation of native structure, post-translational modifications such as glycosylation and phosphorylation [50], and proper functionality. In contrast, bacterially expressed proteins lack glycosylation and phosphorylation moieties, and are often misfolded during purification. As target proteins contain a GST fusion tag, the arrays are always processed for the post-spotting quality control by using an anti-GST antibody with a concentration gradient of GST spots as a standard. This procedure makes it possible to quantify the exact amount of proteins deposited in each spot, and thereby minimizes the inter-lot variability of the results. Furthermore, each subarray contains a series of built-in control spots.

Protein microarray also has another technical limitation attributable to the avidity of protein–protein interaction. The probing and rigorous washing procedure detects mostly the direct protein–protein interaction supported by the stable binding ability. It could not efficiently detect weak and transient protein–protein interactions, or indirect interactions that require accessory molecules or intervening cofactors. In addition, protein microarray screening does not consider the specific subcellular location where the protein–protein interaction actually takes

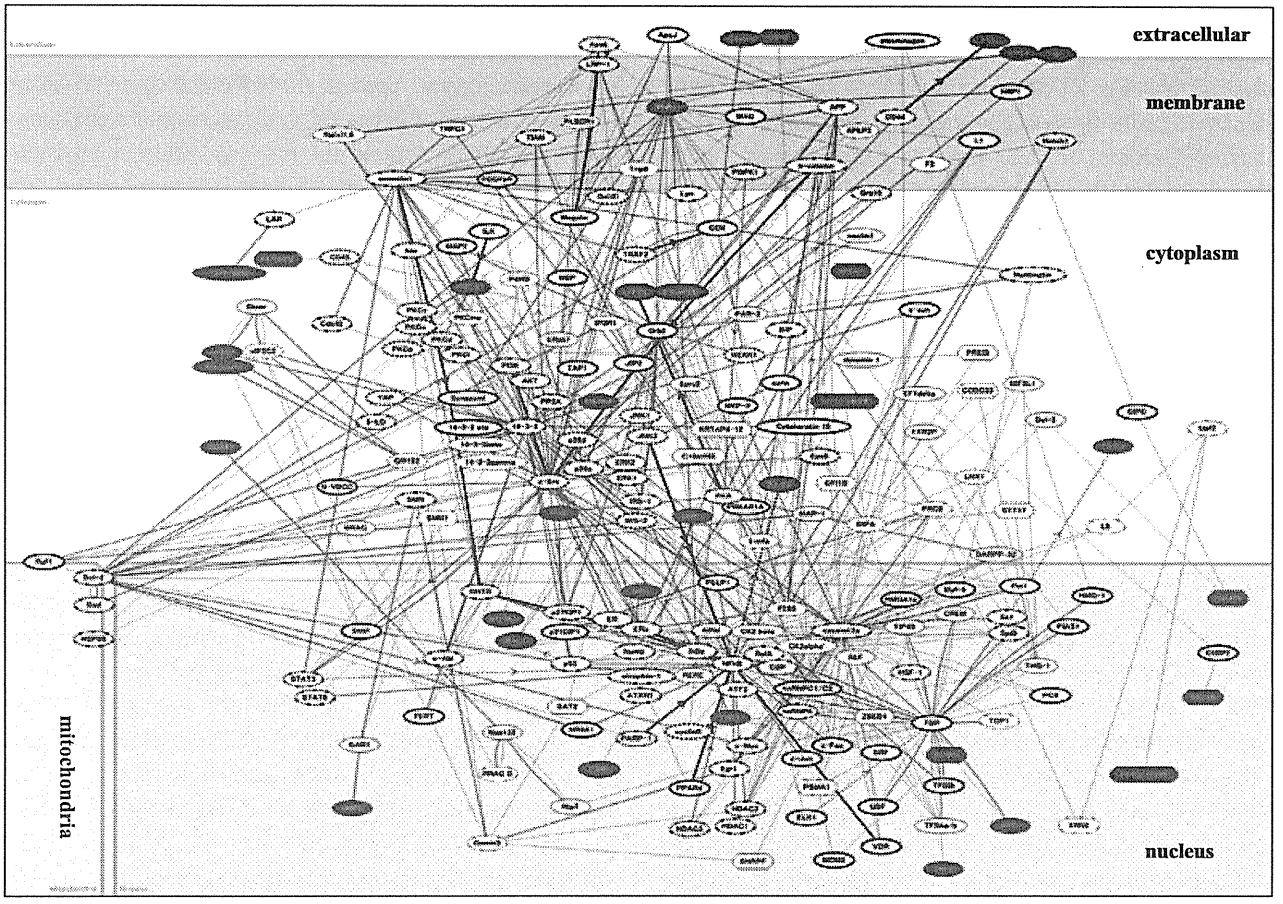

Figure 7. Molecular network of PrPC and the interactors. By importing the list of Entrez gene IDs of 47 PrPIPs, KeyMolnet extracted 39 genes directly linked to 47 PrPIPs. Subsequently, the 'N-points to N-points' search starting from PrPC ending with 39 genes generated a complex molecular network composed of 214 fundamental nodes and 579 molecular relations. They are arranged according to the predicted subcellular location. The red node indicates PrPC on the cell-surface membrane as the starting point, while blue nodes represent PrPIPs listed in Table 1. The connections of thick lines represent the core contents, while thin lines indicate the secondary contents of KeyMolnet. The molecular relation is indicated by dash line with arrow (transcriptional activation), solid line with arrow (direct activation) or solid line without arrow (direct interaction or complex formation).

place. Thus, it is possible that some promiscuous partners are detected, whereas some of the biologically important interactors *in vivo* are left beyond identification. Therefore, protein microarray data always require the validation by other independent methods such as coimmunoprecipitation, far Western blotting, the Y2H screening and so on. Post-translational modifications play a pivotal role in a range of protein–protein interactions. Immunolabelling of the array we utilized with anti-phosphotyrosine antibody showed that approximately 10–20% of the proteins on the array are phosphorylated (Invitrogen, unpubl. data). When the array was utilized for kinase substrate identification, most of known kinases immobilized on the array are enzymatically active with the capacity for autophosphorylation, suggesting that they are functionally active with preservation of proper conformation (data of Invitrogen).

Validation of interaction and colocalization of PrPC with four neuronal PrPC interactors by immunoprecipitation and cell imaging analysis

We selected four PrPIPs for further biochemical characterization, including FAM64A, HOXA1, PLK3 and MPG, because of their potential involvement in neural function. Furthermore, we identified the expression of all of these in differentiated human neurones NTera2N by RT-PCR. FAM64A is a 26-kDa protein with a DUF1466 domain in its N-terminal region. Currently, its biological function

remains unknown. However, the database search on Entrez UniGene, the organized view of the transcriptome, showed that the FAM64A transcript is expressed abundantly in brain tissues, glioma and primitive neuroectodermal tumours. HOXA1 acts as a transcription factor that regulates the proper arrangement of hindbrain segments during development [51]. Homozygous truncating mutations in the human HOXA1 gene disrupt brainstem, inner ear, cardiovascular and cognitive development in patients with the Bosley–Salih–Alorainy syndrome [52]. PLK3 is a member of the polo family serine/threonine kinases that regulate the onset of mitosis and M-phase progression in cell cycle. Long-term potentiation enhances PLK3 expression in hippocampal neurones, suggesting a role of PLK3 in synaptic plasticity [53]. MPG is a DNA repair enzyme that removes mutagenic alkylation adducts of purines from damaged DNA. Astrocytoma cells express a great amount of MPG protein, supporting a role of MPG in astrocytic tumorigenesis [54].

The interaction of PR209 with FAM64A, HOXA1, PLK3 and MPG was verified by coimmunoprecipitation and cell imaging in a transient expression system of HEK293 cells. Because the antibodies sufficient for immunoprecipitation with FAM64A, PLK3 and MPG are currently unavailable, we performed immunoprecipitation analysis by using the tag-specific antibodies. Although cultured human neurones, such as NTera2, appear to be preferable for expression of PrPC interactors, we utilized HEK293 cells because of much easier handling and constant expression of tagged recombinant proteins. It is worth noting that in preliminary experiments, we found that there exists a small but discernible level of interaction between endogeneous PrPC and HOXA1 in adult human brain tissue homogenates (data not shown).

PrPC is structurally separated into two distinct segments composed of the N-terminal flexibly disordered tail (amino acid residues 23–121) that includes the octapeptide repeat region, and the C-terminal globular domain (amino acid residues 121–230) that contains three α-helices and two short anti-parallel β-sheets [55]. The immunoprecipitation study showed that HOXA1 interacts exclusively with the C-terminal half of PR209.

PrPC interactors play a role in nuclear function

Although PrPC is a glycosylphosphatidylinositol (GPI)-anchored cell-surface protein, we found that DsRed-tagged PR209 with the C-terminal GPI anchor site of amino acid residue 231 is located predominantly in the nucleus and the cytoplasm, and less abundantly on the plasma membrane. A recent study showed that PrPC after cleavage of both N-terminal and C-terminal signal peptides is located chiefly in the nucleus, where it interacts with chromatin in neural cell lines [56], supporting our findings that PrPC could interact with its partners in both the nucleus and the cytoplasm. PrPC has two cryptic nuclear localization signals in the N-terminal domain [57]. Nuclear localization of PrPSc-like protein is identified in prion-infected cells [58]. Furthermore, defined populations of neurones express PrPC in their cytoplasm [59]. In the present study, FAM64A, HOXA1 and MPG were located predominantly in the nucleus, where they coexisted with PR209. The involvement of PrPC and interactors in nuclear function is supported by functional annotation on the DAVID database that suggested a major role of PrPIPs in the recognition of nucleic acids. We could categorize the nucleic acid-binding PrPIPs into two distinct groups: (i) proteins involved in RNA splicing, silencing and metabolism: SCNM1, RBM22, DDX47, CWC15, PTRH1, EIF2C1, CIRBP, NOLA2, NOB1 and RNPC3, and (ii) proteins involved in DNA transcription and repair: HOXA1, BAZE2B, MPG, ZNF192, ZNF408, TBPL1, ABT1, ZNF740 and WDR5. Importantly, a previous study indicated that PrPC plays a key role in nucleic acid metabolism by its nucleic acid chaperoning activity [60]. Because protein microarray analysis utilized the recombinant PR209 highly purified from the culture supernatant as a probe, the possibility is unlikely that any contaminating cellular nucleic acids mediate the interaction between PrPC and PrPIPs.

Previous studies showed that PrPC spanning amino acid residues 23–230 designated CyPrP accumulates in the cytoplasm, where it is converted into the PrPSc-like proteinase K-resistant protein (PrP^{RES}) with potent neurotoxicity, when the proteasome activity is suppressed [61,62]. In contrast, we showed that coexpression of large amounts of PR209 with HOXA1 or FAM64A did not generate PrP^{RES} in HEK293 cells, even after exposure of the cells to MG-132. Our observations suggest that both HOXA1 and FAM64A do not act as the chaperone 'protein X' that promotes protein conformational conversion from PrPC to PrPSc at least in a short incubation time of 48 h. Because prion diseases develop after a long incubation period, our observations do not exclude the possibility that a long-term incubation of PrPC and the interactors with some additional cofactors could accelerate the conforma-

tional conversion from PrPC to PrPSc. In addition, we unexpectedly found that PR209 exhibits an intrinsic detergent insolubility in HEK293 cells following transient overexpression. A recent study showed that small amounts of detergent-insoluble prion protein aggregates are present in normal human brains [63].

The molecular network of PrPC and interactors involves key cell signalling pathways

KeyMolnet stores the comprehensive content database that focuses on human molecules and molecular interactions, carefully curated by experts from the literature and public databases [41]. This software makes it possible to effectively extract the most relevant molecular interaction from large quantities of gene expression data, and to establish a biologically relevant logical working model [42]. The present study for the first time by using KeyMolnet, a data-mining tool of bioinformatics, showed that the complex molecular network of PrPC and 47 PrPIPs has a significant relationship with AKT, JNK and MAPK signalling pathways. A previous study showed that PrPC activates diverse signalling pathways involving Fyn, PI3 kinase/Akt, cAMP-dependent protein kinase A and MAP kinase, all of which contribute to neurite outgrowth and neuronal survival in primary culture of mouse neurones [64]. PrPC-knockout mice show exacerbation of ischaemic brain injury, accompanied by reduced expression of Ser473-phosphorylated Akt and increased activities of ERK-1/–2, STAT-1 and caspase-3 in the brain [65,66]. A synthetic peptide PrP106–126 induces neuronal apoptosis in primary cultures of mouse neurones via the JNK-c-Jun pathway [67]. All of these observations suggest a crucial link between the biological function of PrPC and signalling pathways mediated by AKT, JNK and MAPK.

Previously, we showed that the genes located in the Ras/Rac signalling pathway, pivotal for cell proliferation, differentiation and survival, were aberrantly regulated in cultured fibroblasts of PrPC-deficient mice [68]. More recently, by analysing a DNA microarray containing 12 814 human genes, we identified 33 genes differentially expressed between a stable PrPC-expressing HEK293 cell line and the parent PrPC-non-expressing cells [37]. They included 18 genes involved in neuronal and glial functions, five related to production of the extracellular matrix, and two located in the complement cascade. These observations suggest that aberrant expression of PrPC, either overexpression or underexpression, affects a wide range of cell signalling pathways. Most recently, we showed that the zeta isoform of 14-3-3 protein, a scaffold protein on which diverse signal components converge, forms a molecular complex with PrPC and heat shock protein Hsp60 in the human CNS neurones under physiological conditions [23]. This raises the hypothesis that the multimolecular complex is disrupted in the pathological process of prion diseases, resulting in the release of 14-3-3 from degenerating neurones into the cerebrospinal fluid. Unfortunately, the protein microarray utilized in the present study does not include 14-3-3 zeta, Hsp60 or PrPC as targets.

In conclusion, protein microarray is a useful tool for systematic screening and comprehensive profiling of the human PrPC interactome. The great majority of PrPIPs are annotated as the proteins involved in the recognition of nucleic acids. Thus, individual PrPIPs possibly act as regulators of RNA splicing, silencing, and metabolism and modulators for DNA transcription and repair in neural and non-neural cells. Furthermore, the human PrPC–PrPIP network on the whole plays a pivotal role in signalling pathways essential for regulation of cell survival, differentiation, proliferation and apoptosis. These observations propose a logical hypothesis that the dysregultion of PrPC interactome might induce extensive neurodegeneration ongoing in prion diseases, and warrant further studies to clarify the implication of PrPC and the interactors in cellular signalling and nuclear function.

Acknowledgements

This work was supported by the Grant-in-Aid for Scientific Research, the Ministry of Education, Culture, Sports, Science and Technology, Japan (B18300118), the grants from Research on Psychiatric and Neurological Diseases and Mental Health, the Ministry of Health, Labour and Welfare of Japan (H17-020) and Research on Health Sciences Focusing on Drug Innovation, the Japan Health Sciences Foundation (KH21101), and the Nakatomi Foundation.

References

1 Prusiner SB. Prions. *Proc Natl Acad Sci USA* 1998; **95**: 13363–83
2 Aguzzi A, Polymenidou M. Mammalian prion biology: one century of evolving concepts. *Cell* 2004; **116**: 313–27

3 Bendheim PE, Brown HR, Rudelli RD, Scala LJ, Goller NL, Wen GY, Kascsak RJ, Cashman NR, Bolton DC. Nearly ubiquitous tissue distribution of the scrapie agent precursor protein. *Neurology* 1992; **42**: 149–56

4 Telling GC, Scott M, Mastrianni J, Gabizon R, Torchia M, Cohen FE, DeArmond SJ, Prusiner SB. Prion propagation in mice expressing human and chimeric PrP transgenes implicates the interaction of cellular PrP with another protein. *Cell* 1995; **83**: 79–90

5 Kaneko K, Zulianello L, Scott M, Cooper CM, Wallace AC, James TL, Chen FE, Prusiner SB. Evidence for protein X binding to a discontinuous epitope on the cellular prion protein during scrapie prion propagation. *Proc Natl Acad Sci USA* 1997; **94**: 10069–74

6 Büeler H, Fischer M, Lang Y, Bluethmann H, Lipp HP, DeArmond SJ, Prusiner SB, Aguet M, Weissmann C. Normal development and behaviour of mice lacking the neuronal cell-surface PrP protein. *Nature* 1992; **356**: 577–82

7 Manson JC, Clarke AR, Hooper ML, Aitchison L, McConnell I, Hope J. 129/Ola mice carrying a null mutation in PrP that abolishes mRNA production are developmentally normal. *Mol Neurobiol* 1994; **8**: 121–7

8 Sakaguchi S, Katamine S, Nishida N, Moriuchi R, Shigematsu K, Sugimoto T, Nakatani A, Kataoka Y, Houtani T, Shirabe S, Okada H, Hasegawa S, Miyamoto T, Noda T. Loss of cerebellar Purkinje cells in aged mice homozygous for a disrupted PrP gene. *Nature* 1996; **380**: 528–31

9 Graner E, Mercadante AF, Zanata SM, Forlenza OV, Cabral ALB, Veiga SS, Juliano MA, Roesler R, Walz R, Minetti A, Izquierdo I, Martins VR, Brentani RR. Cellular prion protein binds laminin and mediates neuritogenesis. *Mol Brain Res* 2000; **76**: 85–92

10 Lopes MH, Hajj GNM, Muras AG, Mancini GL, Castro RMPS, Ribeiro KCB, Brentani RR, Linden R, Martins VR. Interaction of cellular prion and stress-inducible protein 1 promotes neuritogenesis and neuroprotection by distinct signaling pathways. *J Neurosci* 2005; **25**: 11330–9

11 Schmitt-Ulms G, Legname G, Baldwin MA, Ball HL, Bradon N, Bosque PJ, Crossin KL, Edelman GM, DeArmond SJ, Cohen FE, Prusiner SB. Binding of neural cell adhesion molecules (N-CAMs) to the cellular prion protein. *J Mol Biol* 2001; **314**: 1209–25

12 Chiarini LB, Freitas ARO, Zanata SM, Brentani RR, Martins VR, Linden R. Cellular prion protein transduces neuroprotective signals. *EMBO J* 2002; **21**: 3317–26

13 Brown DR, Qin K, Herms JW, Madlung A, Manson J, Strome R, Fraser PE, Kruck T, von Bohlen A, Schulz-Schaeffer W, Giese A, Westaway D, Kretzschmar H. The cellular prion protein binds copper in vivo. *Nature* 1997; **390**: 684–7

14 Spielhaupter C, Schätzl HM. PrP^C directly interacts with proteins involved in signaling pathways. *J Biol Chem* 2001; **276**: 44604–12

15 Oesch B, Teplow DB, Stahl N, Serban D, Hood LE, Prusiner SB. Identification of cellular proteins binding to the scrapie prion protein. *Biochemistry* 1990; **29**: 5848–55

16 Yehiely F, Bamborough P, Da Costa M, Perru BJ, Thinakaran G, Cohen FE, Carlson GA, Prusiner SB. Identification of candidate proteins binding to prion protein. *Neurobiol Dis* 1997; **2**: 339–55

17 Edenhofer F, Rieger R, Famulok M, Wendler W, Weiss S, Winnacker EL. Prion protein PrP^C interacts with molecular chaperones of the Hsp60 family. *J Virol* 1996; **70**: 4724–8

18 DebBurman SK, Raymond GJ, Caughey B, Lindquist S. Chaperone-supervised conversion of prion protein to its protease-resistant form. *Proc Natl Acad Sci USA* 1997; **94**: 13938–43

19 Stöckel J, Hartl FU. Chaperonin-mediated de novo generation of prion protein aggregates. *J Mol Biol* 2001; **313**: 861–72

20 Zanata SM, Lopes MH, Mercadante AF, Hajj GN, Chiarini LB, Nomizo R, Freitas AR, Cabral AL, Lee KS, Juliano MA, de Oliveira E, Jachieri SG, Burlingame A, Huang L, Linden R, Brentani RR, Martins VR. Stress-inducible protein 1 is a cell surface ligand for cellular prion that triggers neuroprotection. *EMBO J* 2002; **21**: 3307–16

21 Kurschner C, Morgan JI. Analysis of interaction sites in homo- and heteromeric complexes containing Bcl-2 family members and the cellular prion protein. *Mol Brain Res* 1996; **37**: 249–58

22 Mattei V, Garofalo T, Misasi R, Circella A, Manganelli V, Lucania G, Pavan A, Sorice M. Prion protein is a component of the multimolecular signaling complex involved in T cell activation. *FEBS Lett* 2004; **560**: 14–18

23 Satoh J, Onoue H, Arima K, Yamamura T. The 14-3-3 protein forms a molecular complex with heat shock protein Hsp60 and cellular prion protein. *J Neuropathol Exp Neurol* 2005; **64**: 858–68

24 Bragason BT, Palsdottir A. Interaction of PrP with NRAGE, a protein involved in neuronal apoptosis. *Mol Cell Neurosci* 2005; **29**: 232–44

25 Nieznanski K, Nieznanska H, Skowronek KJ, Osiecka KM, Stepkowski D. Direct interaction between prion protein and tubulin. *Biochem Biophys Res Commun* 2005; **334**: 403–11

26 Strom A, Diecke S, Hunsmann G, Stuke AW. Identification of prion protein binding proteins by combined use of far-western immunoblotting, two dimensional gel electrophoresis and mass spectrometry. *Proteomics* 2006; **6**: 26–34

27 Meggio F, Negro A, Sarno S, Ruzzene M, Bertoli A, Sorgato MC, Pinna LA. Bovine prion protein as a modulator of protein kinase CK2. *Biochem J* 2000; **352**: 191–6

28 Fischner MB, Roeckl C, Parizek P, Schwarz HP, Aguzzi A. Binding of disease-associated prion protein to plasminogen. *Nature* 2000; **408**: 479–83

29 Rieger R, Edenhofer F, Lasmézas CI, Weiss S. The human 37-kDa laminin receptor precursor interacts with the prion protein in eukaryotic cells. *Nat Med* 1997; 3: 1283–8
30 Hajj GN, Lopes MH, Mercadante AF, Veiga SS, da Silveira RB, Santos TG, Ribeiro KC, Juliano MA, Jacchieri SG, Zanata SM, Martins VR. Cellular prion protein interaction with vitronectin supports axonal growth and is compensated by integrins. *J Cell Sci* 2007; 120: 1915–26
31 von Mering C, Krause R, Snel B, Cornell M, Oliver SG, Fields S, Bork P. Comparative assessment of large-scale data sets of protein–protein interactions. *Nature* 2002; 417: 399–403
32 Vidalain PO, Boxem M, Ge H, Li S, Vidal M. Increasing specificity in high-throughput yeast two-hybrid experiments. *Methods* 2004; 32: 363–70
33 MacBeath G, Schreiber SL. Printing proteins as microarrays for high-throughput function determination. *Science* 2000; 289: 1760–3
34 Chan SM, Ermann J, Su L, Fathman CG, Utz PJ. Protein microarrays for multiplex analysis of signal transduction pathways. *Nat Med* 2004; 10: 1390–6
35 Schweitzer B, Predki P, Snyder M. Microarrays to characterize protein interactions on a whole-proteome scale. *Proteomics* 2003; 3: 2190–9
36 Satoh J. Protein microarray analysis for rapid identification of 14-3-3 protein binding partners. In *Functional Protein Microarrays in Drug Discovery*. Ed. Predki PF. Boca Raton: CRC Press, 2007; 239–59
37 Satoh J, Yamamura T. Gene expression profile following stable expression of the cellular prion protein. *Cell Mol Neurobiol* 2004; 24: 793–814
38 Satoh J, Nanri Y, Yamamura T. Rapid identification of 14-3-3-binding proteins by protein microarray analysis. *J Neurosci Methods* 2006; 152: 278–88
39 Lein ES, Hawrylycz MJ, Ao N, Ayres M, Bensinger A, Bernard A, Boe AF, Boguski MS, Brockway KS, Byrnes EJ, Chen L, Chen L, Chen TM, Chin MC, Chong J, Crook BE, Czaplinska A, Dang CN, Datta S, Dee NR, Desaki AL, Desta T, Diep E, Dolbeare TA, Donelan MJ, Dong HW, Dougherty JG, Duncan BJ, Ebbert AJ, Eichele G, Estin LK, Faber C, Facer BA, Fields R, Fischer SR, Fliss TP, Frensley C, Gates SN, Glattfelder KJ, Halverson KR, Hart MR, Hohmann JG, Howell MP, Jeung DP, Johnson RA, Karr PT, Kawal R, Kidney JM, Knapik RH, Kuan CL, Lake JH, Laramee AR, Larsen KD, Lau C, Lemon TA, Liang AJ, Liu Y, Luong LT, Michaels J, Morgan JJ, Morgan RJ, Mortrud MT, Mosqueda NF, Ng LL, Ng R, Orta GJ, Overly CC, Pak TH, Parry SE, Pathak SD, Pearson OC, Puchalski RB, Riley ZL, Rockett HR, Rowland SA, Royall JJ, Ruiz MJ, Sarno NR, Schaffnit K, Shapovalova NV, Sivisay T, Slaughterbeck CR, Smith SC, Smith KA, Smith BI, Sodt AJ, Stewart NN, Stumpf KR, Sunkin SM, Sutram M, Tam A, Teemer CD, Thaller C, Thompson CL, Varnam LR, Visel A, Whitlock RM, Wohnoutka PE, Wolkey CK, Wong VY, Wood M, Yaylaoglu MB, Young RC, Youngstrom BL, Yuan XF, Zhang B, Zwingman TA, Jones AR. Genome-wide atlas of gene expression in the adult mouse brain. *Nature* 2007; 445: 168–76
40 Dennis G Jr, Sherman BT, Hosack DA, Yang J, Gao W, Lane HC, Lempicki RA. DAVID: database for annotation, visualization, and integrated discovery. *Genome Biol* 2003; 4: R60
41 Sato H, Ishida S, Toda K, Matsuda R, Hayashi Y, Shigetaka M, Fukuda M, Wakamatsu Y, Itai A. New approaches to mechanism analysis for drug discovery using DNA microarray data combined with KeyMolnet. *Curr Drug Discov Technol* 2005; 2: 89–98
42 Satoh J, Illes Z, Peterfalvi A, Tabunoki H, Rozsa C, Yamamura T. Aberrant transcriptional regulatory network in T cells of multiple sclerosis. *Neurosci Lett* 2007; 422: 30–3
43 Butler DA, Scott MRD, Bockman JM, Borchelt DR, Taraboulos A, Hsiao KK, Kingsbury DT, Prusiner SB. Scrapie-infected murine neuroblastoma cells produce protease-resistant prion proteins. *J Virol* 1998; 62: 1558–64
44 Lorenz H, Windl O, Kretzschmar HA. Cellular phenotyping of secretory and nuclear prion proteins associated with inherited prion diseases. *J Biol Chem* 2002; 277: 8508–16
45 Satoh J, Kuroda Y. Differential gene expression between human neurons and neuronal progenitor cells in culture: an analysis of arrayed cDNA clones in NTera2 human embryonal carcinoma cell line as a model system. *J Neurosci Methods* 2000; 94: 155–64
46 Vincent B, Paitel E, Saftig P, Frobert Y, Hartmann D, De Strooper B, Grassi J, Lopez-Perez E, Checler F. The disintegrations ADAM10 and TACE contribute to the constitutive and phorbol ester-regulated normal cleavage of the cellular prion protein. *J Biol Chem* 2001; 276: 37743–6
47 Robinson WH, Fontoura P, Lee BJ, de Vegvar HE, Tom J, Pedotti R, DiGennaro CD, Mitchell DJ, Fong D, Ho PP, Ruiz PJ, Maverakis E, Stevens DB, Bernard CC, Martin R, Kuchroo VK, van Noort JM, Genain CP, Amor S, Olsson T, Utz PJ, Garren H, Steinman L. Protein microarrays guide tolerizing DNA vaccine treatment of autoimmune encephalomyelitis. *Nat Biotechnol* 2003; 21: 1033–9
48 Quintana FJ, Hagedorn PH, Elizur G, Merbl Y, Domany E, Cohen IR. Functional immunomics: microarray analysis of IgG autoantibody repertoires predicts the future response of mice to induced diabetes. *Proc Natl Acad Sci USA* 2004; 101: 14615–21
49 Zangar RC, Varnum SM, Bollinger N. Studying cellular processes and detecting disease with protein microarray. *Drug Metab Rev* 2005; 37: 473–87
50 Tennagels N, Hube-Magg C, Wirth A, Noelle V, Klein HW. Expression, purification, and characterization of the cytoplasmic domain of the human IGF-1 receptor using a baculovirus expression system. *Biochem Biophys Res Commun* 1999; 260: 724–8

51 Rossel M, Capecchi MR. Mice mutant for both Hoxa1 and Hoxb1 show extensive remodeling of the hindbrain and defects in craniofacial development. *Development* 1999; **126**: 5027–40
52 Tischfield MA, Bosley TM, Salih MAM, Alorainy IA, Sener EC, Nester MJ, Oystreck DT, Chan WM, Andrews C, Erickson RP, Engle EC. Homozygous HOXA1 mutations disrupt human brainstem, inner ear, cardiovascular and cognitive development. *Nat Genet* 2005; **37**: 1035–7
53 Kauselmann G, Weiler M, Wuff P, Jessberger S, Konietzko U, Scafidi J, Staubli U, Bereiter-Hahn J, Strebhardt K, Kuhl D. The polo-like protein kinases Fnk and Snk associate with a Ca^{2+}- and integrin-binding protein and are regulated dynamically with synaptic plasticity. *EMBO J* 1999; **18**: 5528–39
54 Kim NK, Ahn JY, Song J, Kim JK, Han JH, An HJ, Chung HM, Joo JY, Choi JU, Lee KS, Roy R, Oh D. Expression of the DNA repair enzyme, N-methylpurine-DNA glycosylase (MPG) in astrocytic tumors. *Anticancer Res* 2003; **23**: 1417–23
55 Zahn R, Liu A, Lührs T, von Schroetter C, Garcia FL, Billeter M, Calzolai L, Wider G, Wüthrich K. NMR solution structure of the human prion protein. *Proc Natl Acad Sci USA* 2000; **97**: 145–50
56 Crozet C, Vézilier J, Delfieu V, Nishimura T, Onodera T, Casanova D, Lehmann S, Béranger F. The truncated 23–230 form of the prion protein localizes to the nuclei of inducible cell lines independently of its nuclear localization signals and is not cytotoxic. *Mol Cell Neurosci* 2006; **32**: 315–23
57 Gu Y, Hinnerwisch J, Fredricks R, Kalepu S, Mishra RS, Singh N. Identification of cryptic nuclear localization signals in the prion protein. *Neurobiol Dis* 2003; **12**: 133–49
58 Mangé A, Crozet C, Lehmann S, Béranger F. Scrapie-like prion protein is translocated to the nuclei of infected cells independently of proteasome inhibition and interacts with chromatin. *J Cell Sci* 2004; **117**: 2411–16
59 Kovacs GG, Voigtländer T, Hainfellner JA, Budka H. Distribution of intraneuronal immunoreactivity for the prion protein in human prion diseases. *Acta Neuropathol* 2002; **104**: 320–6
60 Gabus C, Auxilien S, Péchoux C, Dormont D, Swietnicki W, Morillas M, Surewicz W, Nandi P, Darlix JL. The prion protein has DNA strand transfer properties similar to retroviral nucleocapsid protein. *J Mol Biol* 2001; **307**: 1011–21
61 Ma J, Wollmann R, Lindquist S. Neurotoxicity and neurodegeneration when PrP accumulates in the cytosol. *Science* 2002; **298**: 1781–5
62 Ma J, Lindquist S. Conversion of PrP to a self-pertuating PrP^{Sc}-like conformation in the cytosol. *Science* 2002; **298**: 1785–8
63 Yuan J, Xiao X, McGeehan J, Dong Z, Cali I, Fujioka H, Kong Q, Kneale G, Gambetti P, Zou WQ. Insoluble aggregates and protease-resistant conformers of prion protein in uninfected human brains. *J Biol Chem* 2006; **46**: 34848–58
64 Chen S, Mangé A, Dong L, Lehmann S, Schachner M. Prion protein as trans-interacting partner for neurons is involved in neurite outgrowth and neuronal survival. *Mol Cell Neurosci* 2003; **22**: 227–33
65 Spudich A, Frigg R, Kilic E, Kilic U, Oesch B, Raeber A, Bassetti CL, Hermann DM. Aggravation of ischemic brain injury by prion protein deficiency: role ERK-1/-2 and STAT-1. *Neurobiol Dis* 2005; **20**: 442–9
66 Weise J, Sandau R, Schwarting S, Crome O, Wrede A, Schulz-Schaeffer W, Zerr I, Bahr M. Deletion of cellular prion protein results in reduced Akt activation, enhanced postischemic caspase-3 activation, and exacerbation of ischemic brain injury. *Stroke* 2006; **37**: 1296–300
67 Carimalo J, Cronier S, Petit G, Peyrin JM, Boukhtouche F, Arbez N, Lemaigre-Dubreuil Y, Brugg B, Miquel MC. Activation of the JNK-c-Jun pathway during the early phase of neuronal apoptosis induced by PrP106-126 and prion infection. *Eur J Neurosci* 2005; **21**: 2311–19
68 Satoh J, Kuroda Y, Katamine S. Gene expression profile in prion protein-deficient fibroblasts in culture. *Am J Pathol* 2000; **157**: 59–68

Received 26 January 2008
Accepted after revision 7 February 2008

Supplementary material

The following supplementary material is available for this article online:

Table S1. Primers utilized for PCR in the present study.
Table S2. The complete list of the proteins immobilized on a human protein microarray utilized in the present study.

The supplementary material is available as part of the online article from: http://www.blackwell-synergy.com/doi/abs/10.1111/j.1365-2990.2008.00947.x

Please note: Blackwell Publishing is not responsible for the content or functionality of any supplementary materials supplied by the authors. Any queries (other than missing material) should be directed to the corresponding author for the article.

Cell Mol Neurobiol (2009) 29:423–438
DOI 10.1007/s10571-008-9338-2

ORIGINAL PAPER

Gene Expression Profiling of Human Neural Progenitor Cells Following the Serum-Induced Astrocyte Differentiation

Shinya Obayashi · Hiroko Tabunoki · Seung U. Kim · Jun-ichi Satoh

Received: 16 August 2008 / Accepted: 10 December 2008 / Published online: 7 January 2009

Abstract Neural stem cells (NSC) with self-renewal and multipotent properties could provide an ideal cell source for transplantation to treat spinal cord injury, stroke, and neurodegenerative diseases. However, the majority of transplanted NSC and neural progenitor cells (NPC) differentiate into astrocytes in vivo under pathological environments in the central nervous system, which potentially cause reactive gliosis. Because the serum is a potent inducer of astrocyte differentiation of rodent NPC in culture, we studied the effect of the serum on gene expression profile of cultured human NPC to identify the gene signature of astrocyte differentiation of human NPC. Human NPC spheres maintained in the serum-free culture medium were exposed to 10% fetal bovine serum (FBS) for 72 h, and processed for analyzing on a Whole Human Genome Microarray of 41,000 genes, and the microarray data were validated by real-time RT-PCR. The serum elevated the levels of expression of 45 genes, including ID1, ID2, ID3, CTGF, TGFA, METRN, GFAP, CRYAB and CSPG3, whereas it reduced the expression of 23 genes, such as DLL1, DLL3, PDGFRA, SOX4, CSPG4, GAS1 and HES5. Thus, the serum-induced astrocyte differentiation of human NPC is characterized by a counteraction of ID family genes on Delta family genes. Coimmunoprecipitation analysis identified ID1 as a direct binding partner of a proneural basic helix-loop-helix (bHLH) transcription factor MASH1. Luciferase assay indicated that activation of the DLL1 promoter by MASH1 was counteracted by ID1. Bone morphogenetic protein 4 (BMP4) elevated the levels of ID1 and GFAP expression in NPC under the serum-free culture conditions. Because the serum contains BMP4, these results suggest that the serum factor(s), most probably BMP4, induces astrocyte differentiation by upregulating the expression of ID family genes that repress the proneural bHLH protein-mediated Delta expression in human NPC.

Keywords Astrocytes · Delta family genes · Human neuronal progenitor cells · ID family genes · Microarray

Abbreviations

NSC	Neural stem cells
NPC	Neural progenitor cells
CNS	Central nervous system
BBB	Blood–brain barrier
bHLH	Basic helix-loop-helix
FBS	Fetal bovine serum
EGF	Epidermal growth factor
bFGF	Basic fibroblast growth factor
LIF	Leukemia inhibitory factor
TGF	Transforming growth factor
RT-PCR	Reverse transcription-polymerase chain reaction
DAVID	Database for annotation visualization and integrated discovery
GO	Gene Ontology
GFAP	Glial fibrillary acidic protein
BMP4	Bone morphogenetic protein 4

S. Obayashi · H. Tabunoki · J.-i. Satoh (✉)
Department of Bioinformatics and Molecular Neuropathology, Meiji Pharmaceutical University, 2-522-1 Noshio, Kiyose, Tokyo 204-8588, Japan
e-mail: satoj@my-pharm.ac.jp

S. U. Kim
Division of Neurology, Department of Medicine, University of British Columbia Hospital, University of British Columbia, Vancouver, BC, Canada

Introduction

Neural stem cells (NSC) with self-renewal and multipotent properties are distributed broadly in the niche of germinal zones in the embryonic and adult mammalian central nervous system (CNS). NSC, unlimitedly propagated in vitro and genetically manipulated ex vivo, could provide an ideal cell source for transplantation to compensate for cell damage in spinal cord injury, stroke, and neurodegenerative diseases (Martino and Pluchino 2006). However, the majority of transplanted NSC and neural progenitor cells (NPC), the cells committed to differentiation into the neuronal lineage, differentiate into astrocytes in vivo under pathological environments in the CNS, which contribute to glial scar formation that inhibits axonal regeneration (Pallini et al. 2005; Ishii et al. 2006). Oxidative stress mediators abundant in pathological lesions elevate the expression of histone deacethylase (HDAC) Sirt1 in mouse NPC, which cooperates with an inhibitory basic helix-loop-helix (bHLH) protein HES1 to mediate epigenetic silencing of a proneural bHLH transcription factor MASH1, leading to astrocyte differentiation of NPC (Prozorovski et al. 2008). To obtain a subset of neurons desirable for cell replacement therapy for human neurological diseases, we should intensively clarify the complex interaction of intrinsic genetic programs and environmental factors that regulate human NSC and NPC proliferation and differentiation. However, at present, molecular mechanisms underlying astrocytic differentiation of human NSC and NPC in vitro and in vivo remain largely unknown.

DNA microarray technology is a powerful approach that allows us to systematically monitor gene expression profile of neural cells during differentiation under development. Microarray analysis showed that neuronal differentiation of human NSC in culture involves the regulation of hundreds of genes, including those essential for Wnt and TGF-beta signaling pathways (Cai et al. 2006). By comparing gene expression profiles between human NPC and differentiated neurons, a previous study identified both PDGF receptor alpha (PDGFRA) and IGF-binding protein 4 (IGFBP4) as key proneural differentiation factors (Yu et al. 2006). A recent study discovered 38 genes expressed commonly between adult and fetal human NPC (Maisel et al. 2007). Recently, we have characterized the DNA damage-responsive gene signature of human astrocytes in culture (Satoh et al. 2006).

Because the serum is a potent inducer of astrocyte differentiation of rodent NSC and NPC in culture (Chiang et al. 1996; Brunet et al. 2004), and the serum components enter the CNS via the disrupted blood–brain barrier (BBB) at the site of CNS injury and ischemia, we studied the effect of the serum on gene expression profile of human NPC in culture by analyzing with a whole genome-scale microarray to identify the gene signature of astrocyte differentiation of human NPC.

Methods

Neural Progenitor Cells in Culture

Cryopreserved human NPC, isolated from the brain of an 18.5-week-old female Caucasian under informed consent, were obtained from Cambrex (Walkersville, MD, USA) as a commercially available product (CC-2599). NPC were plated in a 6-well culture plate coated with polyethyleneimine, and incubated at 37°C in a 5% CO_2/95% air incubator in the NPC medium, composed of the serum-free DMEM/F-12 medium (Invitrogen, Carlsbad, CA, USA) supplemented with a mixture of insulin–transferrin–selenium (ITS) (Invitrogen), 20 ng/ml recombinant human EGF (Higeta, Tokyo, Japan), 20 ng/ml recombinant human bFGF (PeproTech EC, London, UK), and 10 ng/ml recombinant human LIF (Chemicon, Temecula, CA, USA), according to the methods described previously (Carpenter et al. 1999). The half of the medium was renewed every 4 days. Following incubation for several months, NPC in culture continued to proliferate by forming free floating or loosely attached growing spheres. For microarray analysis, nonpassage NPC spheres were harvested, replated in a non-coated 6-well culture plate, and incubated further for 72 h in the NPC medium with or without inclusion of 10% fetal bovine serum (FBS) (Biowest, Miami, FL, USA). In some experiments, NPC were incubated for 72 h in the NPC medium with or without inclusion of 50 ng/ml recombinant human BMP4 (PeproTech).

Human cell lines, such as NTera2 teratocarcinoma, Y79 retinoblastoma, SK-N-SH neuroblastoma, IMR-32 neuroblastoma, U-373MG astrocytoma, HMO6 microglia, HeLa cervical carcinoma, and HepG2 hepatoblastoma, were maintained as described previously (Satoh et al. 2007).

Gene Expression Profiling

Five micrograms of total RNA was isolated from NPC cells by using TRIZOL reagent (Invitrogen). It was in vitro amplified once, and cRNA was processed for microarray analysis on a Whole Human Genome Oligonucleotide Microarray (G4112A, 41,000 genes; Agilent Technologies, Palo Alto, CA, USA), as described previously (Satoh et al. 2006). cRNA prepared from NPC spheres without exposure to the serum (S−) was labeled with a fluorescent dye Cy3, while cRNA of NPC spheres with exposure to the serum (S+) was labeled with Cy5. The array was hybridized at

60°C for 17 h in the hybridization buffer containing equal amounts of Cy3- or Cy5-labeled cRNA. Then, it was scanned by the Agilent scanner (Agilent Technologies). The data were analyzed by using the Feature Extraction software (Agilent Technologies). The fluorescence intensities (FI) of individual spots were quantified following global normalization between Cy3 and Cy5 signals and subsequent Lowess normalization. The ratio of FI of Cy5 signal versus FI of Cy3 signal exceeding 2.0 was defined as significant upregulation, whereas the ratio smaller than 0.5 was considered as substantial downregulation.

Real-Time RT-PCR Analysis

DNase-treated total cellular RNA was processed for cDNA synthesis using oligo(dT)$_{12-18}$ primers and SuperScript II reverse transcriptase (Invitrogen). Then, cDNA was amplified by PCR in LightCycler ST300 (Roche Diagnostics, Tokyo, Japan) using SYBR Green I and primer sets listed in Table 1. The expression levels of target genes were standardized against those of the glyceraldehyde-3-phosphate dehydrogenase (G3PDH) gene detected in parallel in identical cDNA samples. All the assays were performed in triplicate.

Functional Annotation and Molecular Network Analysis

Functional annotation of significant genes identified by microarray analysis was searched by the web-accessible program named Database for Annotation, Visualization and Integrated Discovery (DAVID) version 2008, National Institute of Allergy and Infectious Diseases (NIAID), National Institutes of Health (NIH) (david.abcc.ncifcrf.gov) (Dennis et al. 2003). DAVID covers more than 40 annotation categories, including Gene Ontology (GO) terms, protein–protein interactions, protein functional domains, disease associations, biological pathways, sequence general features, homologies, gene functional summaries, and tissue expressions. By importing the list of the National Center for Biotechnology Information (NCBI) Entrez Gene IDs, this program creates the functional annotation chart, an annotation-term-focused view that lists annotation terms and their associated genes under study. To avoid excessive count of duplicated genes, the Fisher's exact test is calculated based on corresponding DAVID gene IDs by which all redundancies in original IDs are removed.

KeyMolnet is a knowledge-based content database that focuses on relationships among human genes, molecules, diseases, pathways and drugs, which were manually curated by expert biologists (www.immd.co.jp/en/keymolnet/index.html) (Sato et al. 2005). They are categorized into the core contents collected from selected review articles with the highest reliability or the secondary contents extracted from abstracts of PubMed database. The "N-points to N-points" network-search algorithm identifies the molecular network constructed by the shortest route connecting the start point molecules and the end point molecules. The generated network was compared side by side with 346 human canonical pathways of the KeyMolnet library. The algorithm counting the number of overlapping molecular relations between the extracted network and the canonical pathway makes it possible to identify the canonical pathway showing the statistically significant contribution to the extracted network.

Immunohistochemistry

For immunocytochemistry, NPC attached on poly-L-lysine-coated cover glasses were fixed with 4% PFA in 0.1 M phosphate buffer, pH 7.4 at room temperature (RT) for 5 min, followed by incubation with phosphate-buffered saline (PBS) containing 0.5% Triton X-100 at RT for 3 min. After blocking non-specific staining by PBS containing 10% NGS, the cells were incubated at RT for 30 min with a mixture of mouse monoclonal anti-GFAP antibody (GA5; Nichirei, Tokyo, Japan) and rabbit polyclonal anti-nestin antibody (AB5922; Chemicon) or rabbit polyclonal anti-ID1 antibody (C-20; Santa Cruz Biotechnology, Santa Cruz, CA, USA). Then, they were incubated at RT for 30 min with a mixture of Alexa Fluor 488-conjugated anti-rabbit IgG (Invitrogen) and Alexa Fluor 568-conjugated anti-mouse IgG (Invitrogen). After several washes, they were examined on the Olympus BX51 universal microscope.

Western Blot Analysis

To prepare total protein extract, the cells were homogenized in RIPA buffer containing and a cocktail of protease inhibitors (Sigma, St. Louis, MO, USA). Following centrifugation at 12,000 rpm for 10 min at RT, the supernatant was collected and separated on a 12% or 15% SDS–PAGE gel. After gel electrophoresis, the protein was transferred onto nitrocellulose membranes, and the blots were labeled at RT overnight with anti-GFAP antibody (GA5) or anti-ID1 antibody (C-20). Then, they were incubated at RT for 30 min with HRP-conjugated anti-mouse or rabbit IgG (Santa Cruz Biotechnology). The specific reaction was visualized by exposing to a chemiluminescence substrate (Pierce, Rockford, IL, USA). After the antibodies were stripped by incubating the membranes at 50°C for 30 min in stripping buffer, composed of 62.5 mM Tris-HCl, pH 6.7, 2% SDS and 100 mM 2-mercaptoethanol, the blots were processed for relabeling with anti-HSP60 antibody (N-20; Santa Cruz Biotechnology).

Table 1 Primers for PCR for RT-PCR and cloning utilized in the present study

Genes	GenBank accession No.	Sense primers	Antisense primers	Application
NES	NM_006617	5′ctgctcaggagcagcactcttaac3′	5′cttagcctatgagatggagcaggc3′	Real-time RT-PCR
MSI1	NM_002442	5′caaagtgtctatctgggtgtgggc3′	5′acagctgaggcctgcaagcttaca3′	Real-time RT-PCR
GFAP	NM_002055	5′atgaggaggaaggagagaaggggа3′	5′ccttccctttcctgtctgagtctc3′	Real-time RT-PCR
NFH	NM_021076	5′gagaaaggaacatccggaacagcc3′	5′tgggagtgccctctcttgctaaca3′	RT-PCR
MBP	NM_002385	5′gttccggaatcctgtcctcagctt3′	5′taactgttggccggaaattgccgg3′	RT-PCR
ID1	NM_002165	5′aattacgtgctctgtgggtctccc3′	5′gtctctggtgactagtaggtgtgc3′	Real-time RT-PCR
ID1	NM_002165	5′atcatggaagtcgccagtggcagc3′	5′tcagcgacacaagatgcgatcgtc3′	Cloning for luciferase assay
Myc-tagged ID1	NM_002165	5’cggaattccgaaagtcgccagtggcagcac3′	5′gaagatcttctcagcgacacaagatgcgat3′	Cloning for CoIP assay
ID3	NM_002167	5′aacttcgccctgcccacttgactt3′	5′cacctccacgctctgaaaagacct3′	Real-time RT-PCR
NPTX1	NM_002522	5′ttgtcctcatgcacacgaagcagc3′	5′acacgcacacacagatcctctcac3′	Real-time RT-PCR
FOS	NM_005252	5′gagctggtgcattacagagaggag3′	5′ggacttgagtccacacatggatgc3′	Real-time RT-PCR
DLL1	NM_005618	5′acgaatgctgctgaagaggaggga3′	5′aactgtccatagtgcaacggcgac3′	Real-time RT-PCR
MASH1	NM_004316	5′tgagtaaggtggagacactgcgct3′	5′tcagaaccagttggtgaagtcgagaag3′	Real-time RT-PCR
Flag-tagged MASH1	NM_002165	5′cggaattccgaaagctctgccaagatggag3′	5′cgggatcccgtcagaaccagttggtgaagt3′	Cloning for CoIP assay and luciferase assay
G3PDH	NM_002046	5′ccatgttcgtcatgggtgtgaacca3′	5′gccagtagaggcagggatgatgttc3′	Real-time RT-PCR
DLL promoter #1	AF222310	5′ggggtacccctcctgacactaggtggcaaga3′	5′gaagatcttcctcggcctccctccgcctggt3′	Cloning for luciferase assay
DLL promoter #2	AF222310	5′ccgctcgagcggacccctcggctgccgccgcgg3′	5′gaagatcttcggacagcgcggcggcggcgac3′	Cloning for luciferase assay

NES nestin, *MSI1* musashi homolog 1, *GFAP* glial fibrillary acidic protein, *NFH* neurofilament heavy polypeptide, *MBP* myelin basic protein, *ID1* inhibitor of DNA binding 1, *ID3* inhibitor of DNA binding 3, *NPTX1* neuronal pentraxin 1, *FOS* cellular oncogene c-fos, *DLL1* delta-like 1, *MASH1* mammalian achaete scute homolog 1, *G3PDH* glyceraldehyde-3-phosphate dehydrogenase, *CoIP* coimmunoprecipitation. The underlined sequences represent restriction enzyme sites

Coimmunoprecipitation Analysis

The open-reading frame (ORF) of the human ID1 and MASH1 (ASCL1) genes were amplified by PCR using PfuTurbo DNA polymerase (Stratagene, La Jolla, CA, USA) and primer sets listed in Table 1. They were then cloned into the mammalian expression vector pCMV-Myc (Clontech, Mountain View, CA, USA) or p3XFLAG-CMV7.1 (Sigma) to express a fusion protein with an N-terminal Myc or Flag tag. At 48 h after co-transfection of the vectors in HEK293 cells by Lipofectamine 2000 reagent (Invitrogen), the cells were homogenized in M-PER lysis buffer (Pierce) supplemented with a cocktail of protease inhibitors (Sigma). After preclearance, the supernatant was incubated at 4°C for 3 h with rabbit polyclonal anti-Myc-conjugated agarose (Sigma), mouse monoclonal anti-Flag M2 affinity gel (Sigma), or the same amount of normal mouse or rabbit IgG-conjugated agarose (Santa Cruz Biotechnology). After several washes, the immunoprecipitates were processed for Western blot analysis using rabbit polyclonal anti-Myc antibody (Sigma) and mouse monoclonal anti-FLAG M2 antibody (Sigma).

Dual Luciferase Assay

The ORF of the human ID1 gene, amplified by PCR using PfuTurbo DNA polymerase and primer sets listed in Table 1, was cloned into the mammalian expression vector pEF6/V5-His TOPO (Invitrogen) by designing omission of V5 and His tags. The web search on Database of Transcriptional Start Sites (DBTSS; dbtss.hgc.jp) indicated that several E-box (CANNTG) sequences were clustered in the approximately 3,000 bp promoter region of the human DLL1 gene. Two non-overlapping regions of the DLL1 promoter, consisting of the region #1 spanning −1,253 and −254 containing two E-box sequences or the region #2 spanning −2,946 and −1,786 containing 10 E-box sequences, when the first amino acid of the initiation codon is defined as the position zero, were separately amplified by PCR using GC-RICH PCR system (Roche Diagnostics) and primer sets listed in Table 1. They were then cloned into the Firefly luciferase reporter vector pGL4.14-luc2-Hygro (Promega, Madison, WI, USA). The Renilla luciferase reporter vector pGL4.74-hRluc-TK (Promega) was used for an internal control that normalizes variability caused by differences in transfection efficacy. They were co-transfected in HEK293 cells, which were introduced with MASH1 and/or ID1 expression vectors at 36 h before transfection of the luciferase reporter vectors. At 16 h after transfection of the luciferase reporter vectors, cell lysate was processed for dual luciferase assay on a 20/20 Luminometer (Promega). All the assays were performed in triplicate.

Results

Human Neural Progenitor Cells (NPC) in Culture

Human NPC were capable of proliferating for several months by forming free floating or loosely attached growing spheres, when incubated in the NPC medium under the serum-free culture conditions (Fig. 1a). When human NPC spheres were incubated in the NPC medium supplemented with 10% FBS, they rapidly attached on the plastic surface, followed by vigorous outgrowth of a sheet of adherent cells from the attachment face (Fig. 1b). By RT-PCR analysis, NPC cells expressed the transcripts of nestin (NES), musashi homolog 1 (MSI1), and GFAP at high levels, whereas they displayed fairly low levels of NFH and MBP mRNA under culture conditions with or without inclusion of the serum (Fig. 1c, lanes 1–10).

When incubated in the serum-free NPC medium, the great majority of the cells forming the core of NPC spheres exhibited an intense immunoreactivity for nestin, and expressed less intensely immunoreactivity for GFAP (Fig. 2a). In contrast, when incubated in the 10% FBS-containing NPC medium, virtually all of adherent cells with a polygonal shape, growing out from the NPC spheres, expressed very strongly both GFAP and nestin immunoreactivities (Fig. 2b and d–f). None of the cells expressed the oligodendrocyte marker O4 or O1 in the serum-free and serum-containing culture conditions (data not shown). These results suggest that adherent cells growing from NPC spheres at the attachment face represent the cells that underwent astrocyte differentiation.

Upregulated Genes in Human NPC Following Exposure to the Serum

NPC spheres were harvested, replated on a non-coated plastic surface, and incubated further for 72 h in the NPC medium with (S+) or without (S−) inclusion of 10% FBS. Then, total cellular RNA was processed for microarray analysis. Exposure of NPC spheres to the serum elevated the levels of expression of 45 genes (Table 2). They include tropomodulin 1 (TMOD1), inhibitor of DNA binding 1 (ID1), connective tissue growth factor (CTGF), Kruppel-like factor 9 (KLF9), inhibitor of DNA binding 3 (ID3), fibroblast growth factor binding protein 2 (FGFBP2), zinc finger protein 436 (ZNF436), transforming growth factor alpha (TGFA), tumor protein D52 (TPD52), sulfatase 1 (SULF1), regulator of G-protein signaling 4 (RGS4), collectin sub-family member 12 (COLEC12), angiotensinogen (AGT), solute carrier family 16, member 9 (SLC16A9), meteorin (METRN), cathepsin H (CTSH), growth arrest and DNA-damage-inducible beta (GADD 45B), sterile alpha motif domain containing 11 (SAMD11),

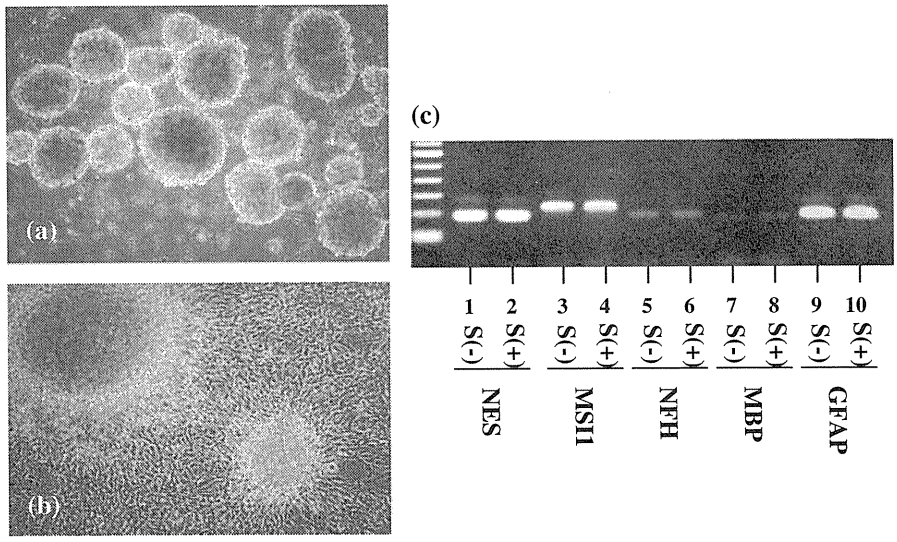

Fig. 1 Human neural progenitor cells (NPC) in culture. **a** Human NPC maintained under the serum-free culture conditions formed free floating growing spheres. **b** Human NPC spheres exposed to 10% FBS rapidly attached on the plastic surface, followed by vigorous outgrowth of a sheet of adherent cells from the attachment face. **a, b** Phase-contrast photomicrographs. **c** RT-PCR amplified for 32 cycles of nestin (NES, lanes 1 and 2), musashi homolog 1 (MSI1, lanes 3 and 4), neurofilament heavy polypeptide (NFH, lanes 4 and 6), myelin basic protein (MBP, lanes 7 and 8), and glial fibrillary acidic protein (GFAP, lanes 9 and 10) expressed in human NPC under the serum-free (S−) and the 10% FBS-containing (S+) culture conditions

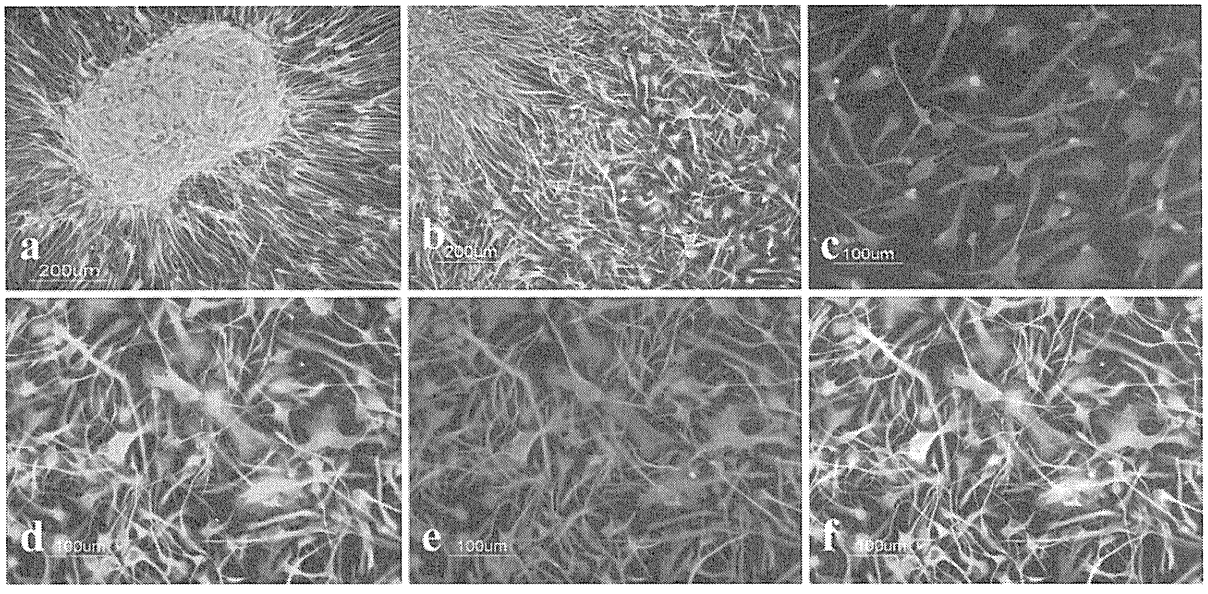

Fig. 2 Nestin, GFAP, and ID1 expression in human NPC in culture. Human NPC spheres attached on poly-L-lysine-coated cover glasses were incubated for 72 h in the NPC medium with (S+) or without (S−) inclusion of 10% FBS, and processed for double-labeling immunocytochemistry for nestin, GFAP, or ID1. **a** S−, NPC sphere, merge of nestin (green) and GFAP (red), **b** S+, vigorous outgrowth of adherent cells from the attachment face of the sphere, merge of nestin (green) and GFAP (red), **c** S+, outgrowth of adherent cells, merge of ID1 (green) and GFAP (red), **d** S+, outgrowth of adherent cells, nestin (green), **e** the same field as **d**, GFAP (red), and **f** merge of **d** and **e**

adenomatosis polyposis coli 2 (APC2), solute carrier family 2 member 5 (SLC2A5), GFAP, coiled-coil domain containing 103 (CCDC103), chromosome 9 open reading frame 58 (C9orf58), chitinase 3-like 2 (CHI3L2), complement factor I (CFI), chemokine C-X-C motif ligand 14 (CXCL14), annexin A1 (ANXA1), regulator of calcineurin 1 (RCAN1), retinal pigment epithelium-specific protein 65 kDa (RPE65), serine/threonine kinase 17a (STK17A), chromosome 4 open reading frame 30 (C4orf30), alpha B crystallin (CRYAB), transmembrane protein 132B (TMEM132B), frizzled homolog 1 (FZD1), inhibitor of DNA binding 2 (ID2), CDC42 effector protein 4